# MULTI-MODE MODEL OF AN AIR HANDLING UNIT FOR THERMAL DEMAND CALCULATIONS IN MODELICA

Philipp Mehrfeld, Moritz Lauster, Kristian Huchtemann, and Dirk Müller
E.ON Energy Research Center, Institute for Energy Efficient Buildings and Indoor Climate,
RWTH Aachen University, Aachen, Germany
pmehrfeld@eonerc.rwth-aachen.de

## ABSTRACT

This paper describes a simulation model to calculate thermal energy demand of air handling units (AHU) centrally installed in buildings with focus on laboratories. The model's design gradually supports energy demand calculations of multiple buildings, e.g. on district level. The AHU is modelled in the open source, object-oriented modelling language Modelica®. The model uses particular operation modes while neglecting dynamic transitions as this reduces computational effort to allow simulations on district level. A comparison of simulation results to experimental results, gained with a test bed at the Institute for Energy Efficient Buildings and Indoor Climate, RWTH Aachen University gives insights into the model's accuracy. The results justify using the model in district simulations, where reduced calculation efforts outweigh acceptable deviations.

Moreover, this paper presents thermal demand simulations of a research site with 195 buildings and a comparison to monitoring data. The computed hourly heating power is satisfying compared to this measured data, e.g. in terms of the coefficient of determination with a value of $R^2 = 0.939$.

## INTRODUCTION

Energy systems for residential as well as non-residential districts provide potential to reduce energy consumption and increase economic efficiency. Thus, a cost-effective approach is to simulate whole districts' energy demands in order to propose optimized solutions. Within a project that focused on two research campuses, simulation results were compared to measured data to verify the simulation models. First attempts revealed an unsatisfactory gap between this data and simulation results. As air handling units (AHU), especially in the context of laboratories, are responsible for a non-negligible part of the districts' energy consumption integrating a model to simulate the AHU's energy demand accurately promised to reduce this gap. Since many buildings of the investigated district are equipped with AHUs, the requirements for the AHU model were to be efficient regarding computational effort and to be able to represent a range of optional functionalities. Therefore, the multi-mode model, represented in Modelica® by so-called state machines, calculates necessary power to provide requested supply air conditions for discrete time steps using static enthalpy based equations. Weather data, which represent tabulated input for the whole simulation environment, describe the outdoor air properties. The supply air passes the building's room, interacts with it and becomes extract air leaving the room. Whilst the AHU model works with time independent equations, the remaining simulation parts like building physics are modelled with its dynamic behaviour.

Furthermore, to characterize the accuracy of the AHU model, experiments on a test bed at the institute were conducted. The AHU model is derived from the test bed's AHU but modelled in a generic way. However, the experiments verify that the developed simulation model is able to determine the thermal power of AHUs within the scope of simplified district simulations.

## AIR HANDLING UNIT

### Construction and functionalities

AHUs have the tasks to supply indoor areas with fresh air that is well tempered, containing a requested humidity, and are free of pollutants (DIN 1946-7, 2009). Figure 1 illustrates a representative component aggregation according to the German pre-standard (DIN V 18599-3, 2011).

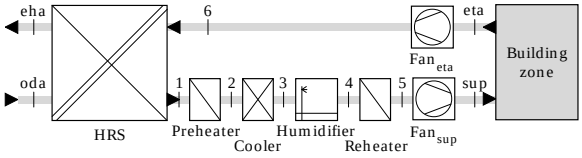


*Figure 1 Schematic of an AHU according to (DIN V 18599-3, 2011)*

Hereby, the following index naming convention is valid throughout the whole paper:

oda, outdoor air;
sup, supply air;
eta, extract air;
eha, exhaust air.

As shown in Figure 1 outdoor air first passes a heat recovery system (HRS) for heat exchange with the extract air coming from the room. Behind that, a preheater is located that operates, e.g. in

humidification mode. Behind this component, a heat exchanger for the purpose of cooling and dehumidification follows, as well as a humidifier. This work focusses on adiabatic humidification, which means a stream of microscopic liquid water particles is injected into the airflow. The particles are quickly absorbed and evaporate while consuming energy from the air with a resulting decrease in temperature. Isothermal humidifiers are not part of the investigations. The following component in Figure 1 is the main heater, the reheater. Behind this the supply air fan follows. Finally, the air flows into the rooms and interacts with the rooms' air volumes. The extract airflow returns out of the building zone, accelerated by the extract air fan, through the HRS and is emitted as exhaust air into the environment.

Usually, one central AHU in a building supplies all connected rooms with conditioned air.

**Thermodynamic basics**

To deal adequately with the energy balances within the AHU's processes, calculations are based on enthalpy flows of moist air. Especially in cases of humidification and dehumidification, this is obviously a necessary approach.

For this purpose, the specific humidity

$$X = \frac{m_{\mathrm{W}}}{m_{\mathrm{dryA}}} = 0.622 \cdot \frac{\varphi \cdot p_{\mathrm{s,W}}(T)}{(p_{\mathrm{W}} + p_{\mathrm{dryA}}) - \varphi \cdot p_{\mathrm{s,W}}(T)} \tag{1}$$

as well as the saturated vapour pressure $p_{\mathrm{s,W}}$ according to the Antoine equation (Antoine, 1888, p. 683 f.; Dimian, 2003, p. 206)

$$p_{\mathrm{s,W}}(T) = 10^{8.07 - \frac{1730.63}{233.43 + \frac{T}{°\mathrm{C}}}} \cdot \frac{101325}{760}\ \mathrm{Pa} \tag{2}$$

represent basic information to describe moist air's condition. Additionally, in dehumidification mode it is necessary to determine the dew point temperature (Sonntag, 1990)

$$T_{\mathrm{dew}}(X) = \frac{243.12\ °\mathrm{C} \cdot \ln A}{17.62 - \ln A} \tag{3}$$

with

$$A = \frac{X \cdot (p_{\mathrm{W}} + p_{\mathrm{dryA}})}{(0.622 + X) \cdot 611.2\ \mathrm{Pa}}. \tag{4}$$

Figure 2 illustrates qualitatively in $h$-$X$-diagrams how states of moist air change depending on the performed process. While during the processes heating (a) and cooling (b) the specific humidity stays the same (in other words, no water mass is added or separated), in the modes humidification (c) and dehumidification (d) the value for specific humidity increases and decreases, respectively. Furthermore, Figure 2 (c) shows that during an adiabatic humidification the air temperature declines, whereas the enthalpy stays constant. For the purpose of dehumidification (see Figure 2 (d)), the steps include cooling, separation of liquid water, and reheating. Thus, dehumidification is obviously an energy consuming procedure.

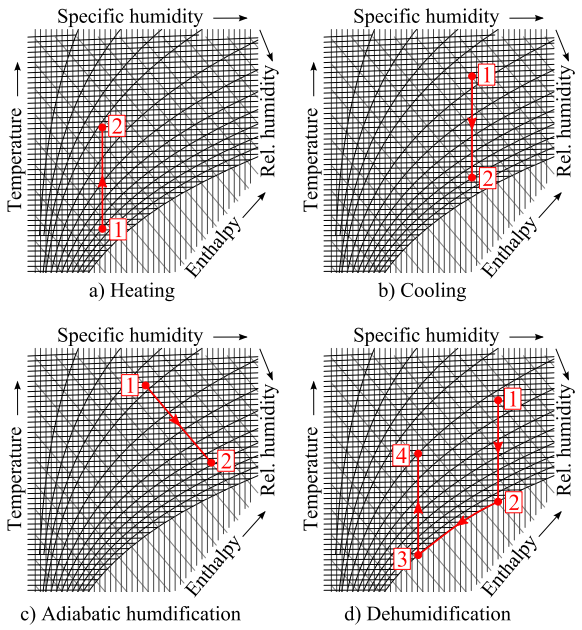


*Figure 2 Change of states of moist air in qualitative h-X-diagrams*

## SIMULATION MODEL

Although the model was built using the modelling language Modelica® for dynamic simulations, for the purpose of saving computational time, all inputs are sampled, assuming them as constant for a defined discrete time step, and further on processed in state machines.

To indicate the heat transfer quality of a HRS, the so-called temperature differential $\phi_t$ (VDI 3803-5, 2013) is part of the AHU model and determined by

$$\phi_t = \frac{T_1 - T_{\mathrm{oda}}}{T_6 - T_{\mathrm{oda}}}. \tag{5}$$

Another important parameter that is considered in the simulation model is the bypass factor (Lindeburg, 2013, p. 38-7 f.)

$$\mathrm{BPF} = \frac{T_3 - T_{\mathrm{surf}}}{T_2 - T_{\mathrm{surf}}} \tag{6}$$

with $T_{\mathrm{surf}} = T_{\mathrm{dew}}$ denoting the surface temperature of the cooler's fins. The BPF takes a certain air mass flow into account that can be seen as not touching the fins' surface and therefore getting bypassed through the cooler.

Air properties, in terms of temperature and humidity, behind the HRS are defined by the known outdoor air conditions and the temperature differential $\phi_t$ (see (5)). Additionally, the properties in position 5 (compare Figure 1) are given values. Therefore, the control volumes in Figure 3 to Figure 7 encompass the range of supply duct from position 1 to 5. The activated components are highlighted. The right-sided graphs in the following figures illustrate qualitatively temperature rises and drops and how to imagine the change of enthalpy. With the help of these graphics the following subsections present the

five possible modes of the AHU model and the formulae that are implemented in the corresponding state machine.

**Only heating**

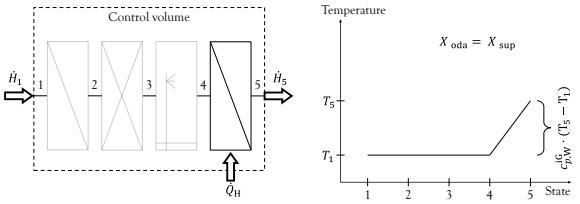


*Figure 3 Only heating*

$$\dot{Q}_{\mathrm{C}} = 0 \tag{7}$$

$$\dot{Q}_{\mathrm{H}} = \dot{m}_{\mathrm{dryA}} \left( c_{p,\mathrm{dryA}}^{\mathrm{iG}} + X_{\mathrm{oda}}\, c_{p,\mathrm{W}}^{\mathrm{iG}} \right) \cdot (T_5 - T_1) \tag{8}$$

**Only cooling**

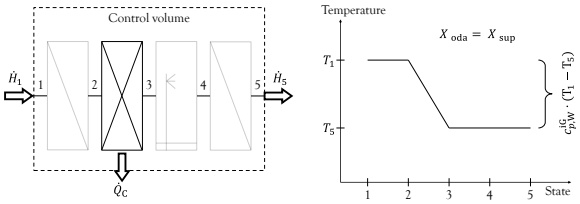


*Figure 4 Only cooling*

$$\dot{Q}_{\mathrm{C}} = \dot{m}_{\mathrm{dryA}} \left( c_{p,\mathrm{dryA}}^{\mathrm{iG}} + X_{\mathrm{oda}}\, c_{p,\mathrm{W}}^{\mathrm{iG}} \right) \cdot (T_1 - T_5) \tag{9}$$

$$\dot{Q}_{\mathrm{H}} = 0 \tag{10}$$

**Dehumidification**

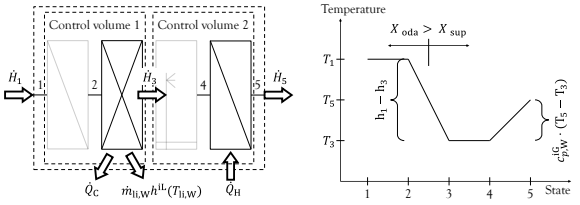


*Figure 5 Dehumidification*

$$\dot{Q}_{\mathrm{C}} = \dot{m}_{\mathrm{dryA}} \left( c_{p,\mathrm{dryA}}^{\mathrm{iG}} + X_{\mathrm{oda}}\, c_{p,\mathrm{W}}^{\mathrm{iG}} \right) \cdot (T_1 - T_3) + \dot{m}_{\mathrm{dryA}} \left( X_{\mathrm{oda}} - X_{\mathrm{sup}} \right) \cdot \Delta h_{\mathrm{V}} \tag{11}$$

$$\dot{Q}_{\mathrm{H}} = \dot{m}_{\mathrm{dryA}} \left( c_{p,\mathrm{dryA}}^{\mathrm{iG}} + X_{\mathrm{sup}}\, c_{p,\mathrm{W}}^{\mathrm{iG}} \right) \cdot (T_5 - T_3) \tag{12}$$

**Humidification plus heating**

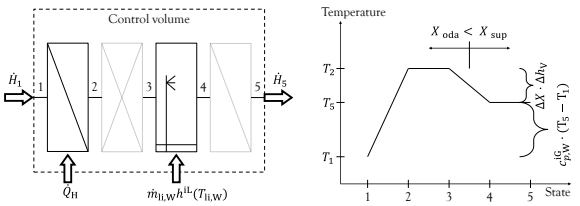


*Figure 6 Humidification plus heating*

$$\dot{Q}_{\mathrm{C}} = 0 \tag{13}$$

$$\dot{Q}_{\mathrm{H}} = \dot{m}_{\mathrm{dryA}} \left( c_{p,\mathrm{dryA}}^{\mathrm{iG}} + X_{\mathrm{oda}}\, c_{p,\mathrm{W}}^{\mathrm{iG}} \right) \cdot (T_5 - T_1) + \dot{m}_{\mathrm{dryA}} \left( X_{\mathrm{sup}} - X_{\mathrm{oda}} \right) \cdot \Delta h_{\mathrm{V}} \tag{14}$$

**Humidification plus cooling**

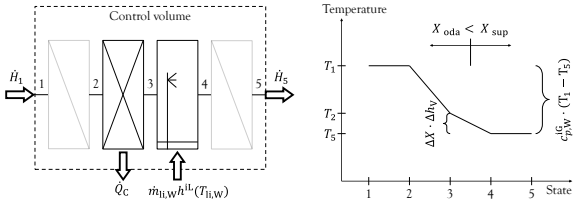


*Figure 7 Humidification plus cooling*

$$\dot{Q}_{\mathrm{C}} = \dot{m}_{\mathrm{dryA}} \left( c_{p,\mathrm{dryA}}^{\mathrm{iG}} + X_{\mathrm{oda}}\, c_{p,\mathrm{W}}^{\mathrm{iG}} \right) \cdot (T_1 - T_5) + \dot{m}_{\mathrm{dryA}} \left( X_{\mathrm{sup}} - X_{\mathrm{oda}} \right) \cdot \Delta h_{\mathrm{V}} \tag{15}$$

$$\dot{Q}_{\mathrm{H}} = 0 \tag{16}$$

Figure 8 displays a flow chart of the decision procedure with its conditions.

Moreover, the HRS is automatically enabled or disabled depending, whether it is worth or not, which is evaluated by comparing $T_{\mathrm{oda}}$ to $T_6$.

## EXPERIMENTAL EXAMINATION

At the E.ON Energy Research Center, Institute for Energy Efficient Buildings and Indoor Climate, RWTH Aachen University, a test bed of an AHU served for experiments to verify the usage of the AHU model for its purpose to approximate thermal power demand of a laboratory's AHU. The test bed provides volume flow rates up to 4000 m³/h and would be able to supply a laboratory area of 160 m² with conditioned air. A rotary heat exchanger represents the HRS. The ductwork has a cross sectional area of 0.65 m². Unfortunately, a humidifier does not exist. In addition, the experimental setup does not provide the emulation of a room load. Thus, the supply airflow becomes extract airflow after 50 m of duct.

The experiment concept is divided in 3 categories:

- Only heating (number 1 to 9)
- Only cooling (number 10 to 13)
- Dehumidification (number 14 to 20)

To gain a satisfactory set of measured data, the mean duration for each experiment was 19 h and was performed under real weather conditions of the outdoor air. The experiments within the categories were altered in terms of HRS activation, volume flow rate, and the preheater's thermal power.

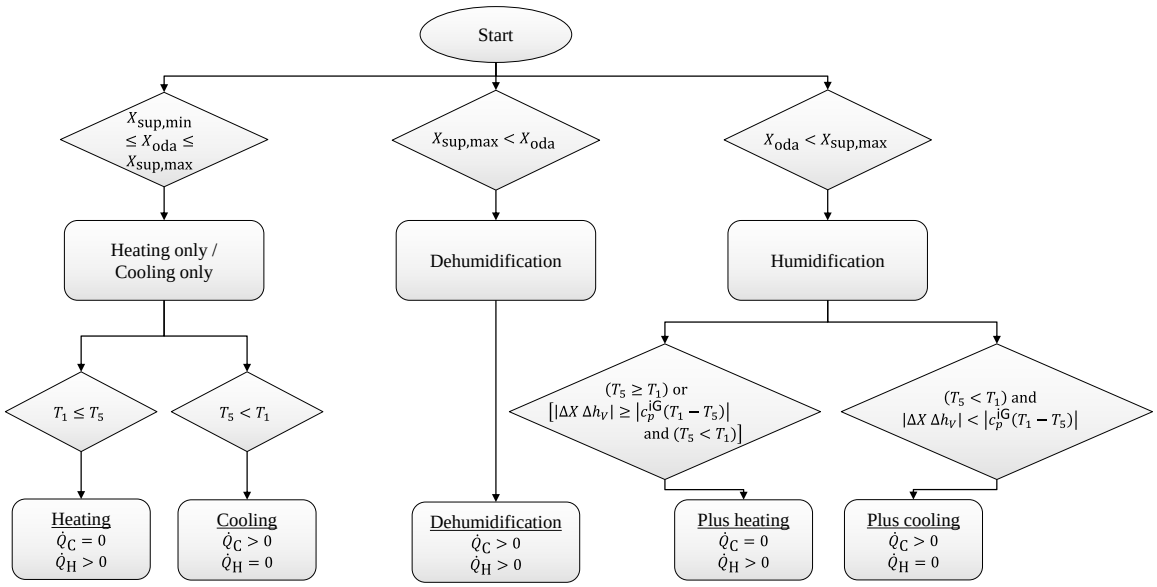


*Figure 8 Flow chart of mode decision procedure*

The values of interest calculated via measured data are the heating and cooling power. In terms of relative deviation, Figure 9 visualises the results for the differences between experimental and simulated energy consumptions related to the experimental energy as reference value.

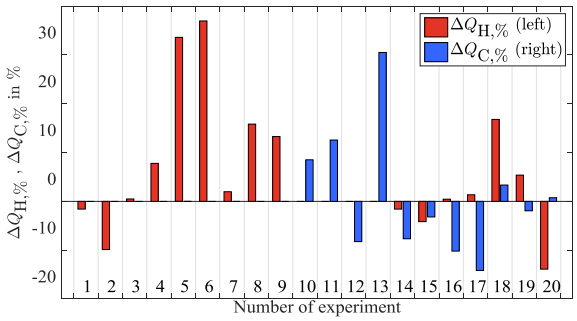


*Figure 9 Relative deviations of heating and cooling energy*

The highest deviations can be observed in experiment 5 and 6. Since both experiments were conducted with the highest volume flow rate of all tests, probably a highly inhomogeneous temperature field was created behind the rotary heat exchanger (VDI 3803-5, 2013). Therefore, the sensors could not detect a representative average temperature and humidity in the duct, which results in inaccurately calculated thermal powers. Furthermore, a significant drop of the relative deviation can be detected from experiment 6 to 7, where the only mentionable modification in the experimental setup was deactivating the rotary heat exchanger. Apparently, whether the rotary heat exchanger is activated or deactivated, has a considerable impact. A similar effect can be seen in the reasonable increase of relative deviation from experiment 12 to 13, as the HRS is enabled in experiment 12 and disabled in experiment 13. Compared to the first category, in this case the cooling energy is the result of interest and thus, the heat in the HRS flows vice versa (from the supply to the extract duct) and this might result in an increasing deviation instead of a decreasing.

Figure 10 and Figure 11 display the measured mean heating and cooling power with their uncertainties of measurement determined according to (JCGM 100, 2008). The figures additionally present the simulation results. As the simulations also use measured values as inputs, in particular outdoor, supply, and extract air temperature and humidity as well as volume flow rate, uncertainties of the simulation results have to be considered, too.

The thermal powers of the experiments are calculated based on monitored data of sensors which are located in the water stream of the heating and cooling circuits that supply the heat exchangers of the AHU test bed. In contrast, the measured data serving as simulation inputs are detected by sensors placed in the air stream. Therefore, the uncertainty ranges of measurement and simulation results are independent.

Regarding the mean thermal power, 13 out of 20 comparisons are within reasonable and valid ranges. However, experiment 5, 6 and 13 do not match due to possible reasons that have already been discussed.

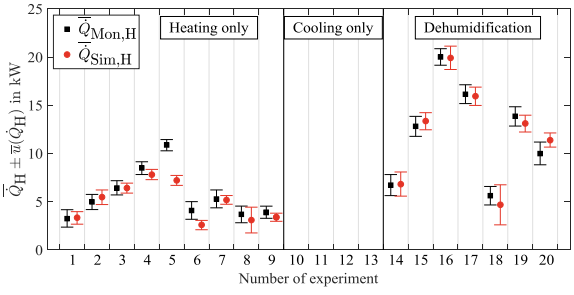


*Figure 10 Measured values and uncertainties for the mean heating power*

Moreover, the simulated results of experiment 8 and 18 show outstandingly high ranges of uncertainties. This is because in these cases the air volume flow rates are the smallest ones and, as a conclusion, come with high uncertainties of measurement since values of the measuring device are near its zero point, which influences the accuracy badly.

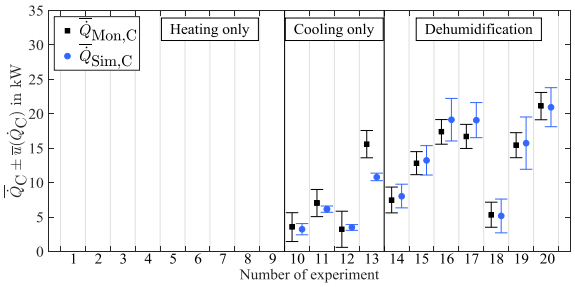


*Figure 11 Measured values and uncertainties for the mean cooling power*

Cooling power in experiment 12 was provided from the water cooling circuit with a comparatively small temperature difference but high volume flow rate. Consequently, this results in a large uncertainty (see Figure 11) since the volume flow rate is a proportionality factor in two terms of the uncertainty calculation. Furthermore, all simulated cooling powers in the dehumidification category have a relatively high range of uncertainty due to an additional term including the enthalpy of evaporation, which does not exist in other equations (see (11)). This is especially noticeable at the result of experiment 19.

## SIMULATIONS

### Simulation setup

The AHU model is centrally integrated in a superior building model (Lauster et al., 2014), which are both part of the open source Modelica® library "AixLib" (*AixLib*, Open Source). The building model has been validated using test setups designed by the ASHRAE Standard Project Committee 140 (ANSI/ASHRAE Standard 140, 2011) as well as via test cases of the German Guideline VDI 6007 (VDI 6007, 2012). This building model is based on the zone principle, i.e., rooms with similar properties are summarised to zones. The building physics encompass windows, outer and inner walls as well as homogeneously assumed room air volumes for each zone. Additionally, the walls consider the heat capacity of the building mass. Furthermore, the simulation model contains all three fundamental types of heat transfer mechanisms: conduction, convection, and radiation. Besides tabulated weather data, models to determine internal gains are also part of the simulation setup. Every zone is optionally equipped with an ideally modelled heater and cooler. Apart from this conventional insertion or extraction of heat, the central AHU provides mechanical ventilation for selected zones. The AHU is fed via tabulated data in terms of desired supply air temperature, air volume flow rate, minimal and maximal humidity.

Whereas the AHU model operates with sampled, hence for a defined time period constant values, the remaining simulation models handle equations dynamically.

### District wide analysis

Overall aim and reason for creating the AHU model was to close the gap between monitoring and simulated data of a whole research district. Therefore, two district wide simulations were performed, one without the AHU model and one including AHUs that supply the laboratory zones in several buildings. The use case is a non-residential district near Aachen, Germany, that consists of 195 buildings with institutions in the field of chemistry, natural and engineering science. Diverse AHU parameters were assumed based on literature (VDI 2071, 1997; Lindeburg, 2013; SIA 2024, 2006) as well as perceptions from the experiments (Mehrfeld, 2014). Figure 13 displays the consumed heating power over time for 2013 for the simulations with and without using an AHU model. Since monitoring data is shown as well, the benefit due to the AHU model is qualitatively visible in Figure 13.

To quantify the quality of simulated data compared to measured data, the statistical approaches of linear regression as well as the coefficient of determination $R^2$ are chosen. Every value $y_i$, in the scope of this paper the thermal power, can be described by a constant offset $\beta_0$, a coefficient $\beta_1$, an error variable $\varepsilon_i$ and the measured $i^{\mathrm{th}}$ data point $x_i$ according to

$$y_i = \beta_0 + \beta_1 \cdot x_i + \varepsilon_i. \tag{17}$$

Besides the exact description shown in (17), a prediction $\hat{y}_i$ can be made with the deviation of the error term $\varepsilon_i$:

$$\hat{y}_i = \beta_0 + \beta_1 \cdot x_i \tag{18}$$

From the set of data points the offset $\beta_0$ and coefficient $\beta_1$ can be determined. The less deviation this straight line according to (18) has compared to the angle bisector the better the prediction, or in this case the simulated thermal power.

In terms of characterising the grade of the correlation, the coefficient of determination $R^2$ fulfils this demand. $R^2$ follows the equation

$$R^2 = 1 - \frac{\sum_{i=1}^{N}(y_i - \hat{y}_i)}{\sum_{i=1}^{N}(y_i - \bar{y})}, \tag{19}$$

where $y_i$ denotes a measured value and $\bar{y}$ the arithmetic mean of all measured values.

Figure 12 illustrates the results of the linear regression analysis including the coefficient of determination $R^2$ for a district wide simulation with AHU compared to the monitoring data (mean daily values).

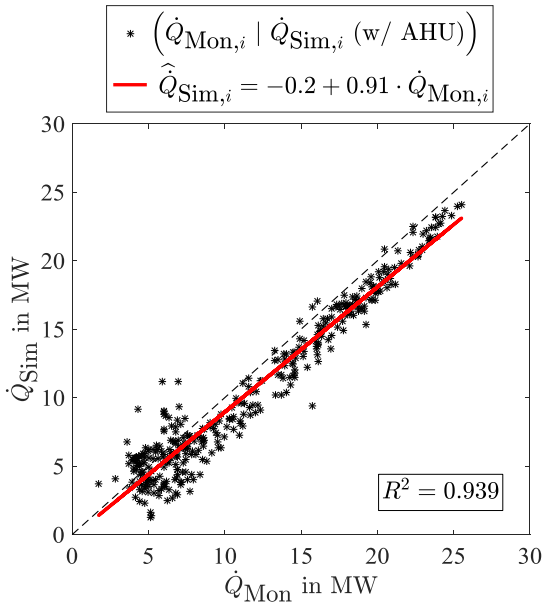


*Figure 12 Linear regression analysis of the district simulation*

It should be clarified that deviations possibly result due to inconsistently metered data and assumptions that had to be made regarding buildings' physics, AHU, and other parameters.

**Influences of AHU parameters**

Beyond creating an AHU model, examining this experimentally and simulating a whole research district, influences of the parametrisation of the AHU model based on the annual thermal energy consumption of three exemplary buildings were investigated. For this purpose the parameters BPF, $\phi_t$, and the minimal humidity threshold $X_{\mathrm{sup,min}}$ as well as the maximal one $X_{\mathrm{sup,max}}$ were altered. According to (Lindeburg, 2013, p. 38-7 f.) the selected range was $\mathrm{BPF} = 0.10 \ldots 0.35$. Regarding the specific humidity thresholds, i.e., when dehumidification or humidification mode is activated, were varied within $\left(X_{\mathrm{sup,min}} \mid X_{\mathrm{sup,max}}\right) = (6.5 \mid 6.0)$ g/kg ... $(7.0 \mid 10.0)$ g/kg according to (DIN V 18599-3, 2011) and (SIA 2024, 2006). Concerning the temperature differential this work differs between values for activated HRS $\phi_{t,\mathrm{act}}$ and deactivated HRS $\phi_{t,\mathrm{deact}}$. Since observations during the experiments have shown that even with disabled rotary heat exchanger heat is transferred through the HRS, this effect can be taken into account via $\phi_{t,\mathrm{deact}}$. The chosen set for the pairing of $\phi_t$ was $\left(\phi_{t,\mathrm{deact}} \mid \phi_{t,\mathrm{act}}\right) = (0.2 \mid 0.8)$ ... $(0.4 \mid 0.6)$ based on (VDI 2071, 1997) and (Mehrfeld, 2014). Whilst the first pairing represents a good HRS, the second one is a bad HRS. Table 1 displays the resulting mean relative differences related to a reference simulation in terms of thermal energies $\Delta\bar{Q}_{\mathrm{H/C,\%}}$. To gain these results all possible parameter combinations were simulated.

*Table 1*
*Quantitative impact of parameter variation*

| Parameter | $\Delta\bar{Q}_{\mathrm{H,\%}}$ in % | $\Delta\bar{Q}_{\mathrm{C,\%}}$ in % |
|---|---|---|
| BPF | 10.2 | 12.0 |
| $X_{\mathrm{sup,min/max}}$ | -34.5 | -47.7 |
| $\phi_{t,\mathrm{deact/act}}$ | 23.3 | 4.7 |

## CONCLUSION

Within this work a multi-mode model of an air handling unit (AHU) was created using the open source, object-oriented modelling language Modelica®. Whereas the state machines of the AHU model operate statically, the superior building model as well as weather influences simulate dynamically. As the model should be part of district wide building simulations, the aim is to keep computational effort in a moderate range while gaining reasonable results. All models are part of the open source Modelica® library "AixLib" (*AixLib*, Open Source).

At the institute's AHU test bed 20 experiments were conducted to characterise the model's accuracy. The verification revealed discrepancies between simulation and experimental results with a mean deviation of 8.25 % and a relatively high standard deviation of 13.53 percentage points. Nevertheless, this results justify using the model in district simulation, where reduced calculation efforts outweigh acceptable deviations.

Regarding simulations of a research district including 195 buildings the benefit could clearly be observed (see Figure 13) and quantified in terms of the coefficient of determination with a value of $R^2 = 0.939$.

Furthermore, a brief sensitivity analyses was performed by altering important parameters, in particular the cooler's bypass factor, the allowed humidity range and the efficiency of the heat recovery device. Table 1 shows an overview of the analysis' results and reveals the supply air humidity as most influencing factor, which is due to the high heating and cooling power consumed in dehumidification mode.

Unfortunately, within the scope of this paper computational time savings were not quantified. Moreover, as no comparable dynamically working AHU model was available, differences in thermal power demand due to neglecting transient effects could not be investigated.

However, the paper presents a multi-mode AHU model that can be easily implemented in Modelica® simulation environments. Simple parametrisation as well as clarity about operating modes are advantages of this AHU model. Besides the shown improvement in district wide simulations that comes along with using the AHU model, this component can in general be used in similar applications, where simplicity and level of detail have to compromise.

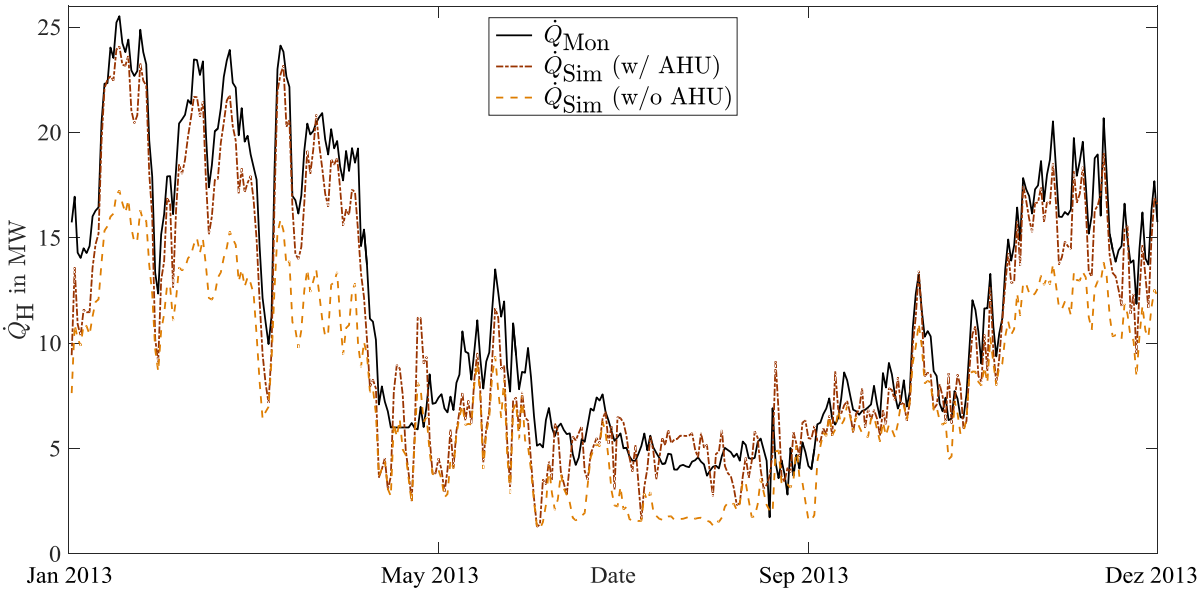


*Figure 13 District wide heat power consumption*

## NOMENCLATURE

| | |
|---|---|
| $\beta_0$, | offset of linear regression; |
| $\beta_1$, | coefficient of linear regression; |
| $\Delta$, | difference; |
| $\varepsilon$, | error variable; |
| $\varphi$, | relative humidity; |
| $\phi_t$, | temperature differential; |
| act, | activated; |
| AHU, | air handling unit; |
| BPF, | bypass factor; |
| $c_p$, | specific heat capacity at constant pressure; |
| C, | cooling; |
| deact, | deactivated; |
| dew, | dew point; |
| dryA, | dry air; |
| eha, | exhaust air; |
| eta, | extract air; |
| $h$, | specific enthalpy; |
| $\Delta h_{\mathrm{V}}$, | specific enthalpy of vaporization; |
| H, | heating; |
| $\dot{H}$, | enthalpy flow rate; |
| HRS, | heat recovery system; |
| $i$, | number of data point; |
| iG, | ideal gas; |
| iL, | ideal liquid; |
| li, | liquid; |
| $m$, | mass; |
| $\dot{m}$, | mass flow rate; |
| max, | maximal; |
| min, | minimal; |
| Mon, | monitoring data; |
| $N$, | amount of data points; |
| oda, | outdoor air; |
| $p$, | (partial) pressure; |
| $Q$, | heat (energy); |
| $\dot{Q}$, | heat flow rate; |
| $R^2$, | coefficient of determination; |
| s, | saturated; |
| Sim, | simulation/simulated; |
| sup, | supply air; |
| surf, | surface; |
| $T$, | temperature; |
| $\bar{u}$, | mean uncertainty of measurement; |
| W, | water; |
| $x$, | measured value; |
| $y$, | simulated value; |
| $\bar{y}$, | arithmetic mean value; |
| $\hat{y}$, | predicted value; |
| $X$, | specific humidity. |

## REFERENCES


ANSI/ASHRAE Standard 140:2011. Standard Method of Test for the Evaluation of Building Energy Analysis Computer Programs. American Society of Heating, Refrigerating and Air-Conditioning Engineers, Inc., 2011.

Antoine, C., 1888. Comptes rendus hebdomadaires des séances de l'Académie des sciences: Tensions des vapeurs, nouvelle relation entre les tensions et les températures. L'Académie des sciences, Frankreich.

VDI 2071:1997-12. Heat recovery in heating, ventilation and air conditioning plants. ICS: 91.140.30. Association of Engineers. Beuth Verlag GmbH, Berlin, 1997.

VDI 6007:2012-03. Calculation of transient thermal response of rooms and buildings. ICS: 91.120.10, 91.140.10. Association of Engineers. Beuth Verlag GmbH, Berlin, 2012.

VDI 3803-5:2013-04. Air-conditioning, system requirements - Heat recovery systems (VDI Ventilation Code of Practice).

ICS: 91.140.30. Association of Engineers. Beuth Verlag GmbH, Berlin, 2013.

Dimian, A.C., 2003. Integrated Design and Simulation of Chemical Processes, 1st ed. ISBN: 9780080534800. Elsevier Science, Amsterdam.

DIN 1946-7:2009-07. Ventilation and air conditioning - Part 7: Venitlation systems in laboratories. ICS: 91.140.30. DIN German Institute for Standardization. Beuth Verlag GmbH, Berlin, 2009.

DIN V 18599-3:2011-12. Energy efficiency of buildings - Calculation of the net, final and primary energy demand for heating, cooling, ventilation, domestic hot water and lighting - Part 3: Net energy demand for air conditioning. ICS: 91.140.30. DIN German Institute for Standardization. Beuth Verlag GmbH, Berlin, 2011.

Lauster, M., Teichmann, J., Fuchs, M., Streblow, R., Mueller, D., 2014. Low order thermal network models for dynamic simulations of buildings on city district scale. Building and Environment, pp. 223–231. DOI: 10.1016/j.buildenv.2013.12.016.

Lindeburg, M.R., 2013. Mechanical Engineering Reference Manual for the PE Exam, 13th ed. ISBN: 9781591264149. Professional Publications, Inc., Belmont.

Mehrfeld, P., 2014. Experimental Investigation of Air Handling Units in Laboratories. (Master Thesis, unpublished). RWTH Aachen University, E.ON Energy Research Center, Institute for Energy Efficient Buildings and Indoor Climate, Aachen, Germany.

AixLib, 0.2.1. RWTH Aachen University, E.ON Energy Research Center, Institute for Energy Efficient Buildings and Indoor Climate, Aachen, Germany. https://github.com/RWTH-EBC/AixLib.

Sonntag, D., 1990. Important new Values of the Physical Constants of 1986: Vapour Pressure Formulations based on ITS-90, and Psychrometer Formulae, in: Z. Meteorol, vol. 40, pp. 340–344.

SIA 2024:2006. Standard-Nutzungsbedingungen für die Energie- und Gebäudetechnik. Swiss Society of Engineers and Architects, 2006.

JCGM 100:2008. Evaluation of measurement data - Guide to the expression of uncertainty in measurement. Working Group 1 of the Joint Committee for Guides in Metrology, 2008. http://www.bipm.org/utils/common/documents/jcgm/JCGM_100_2008_E.pdf.